Collective π-electronic excitations in BN double-walled nanotubes

Vl. A. Margulis*
Department of Physics, Mordovian Ogarev State University, Saransk 430000, Russia

E. E. Muryumin and E. A. Gaiduk
Department of Chemistry, Mordovian Ogarev State University, Saransk 430000, Russia
(Received 27 May 2008; published 9 July 2008)

We report a systematic theoretical study of the collective π-electronic excitations in boron nitride double-walled nanotubes (BN-DWNTs). For simplicity, it is assumed that both shells (inner and outer) of such tubes have a zigzag achiral structure. Taking into account intershell Coulomb coupling and neglecting intershell electron tunneling, we introduce the effective dynamic-dielectric-response function of the BN-DWNTs, which depends on frequency ω, wave number q, and angular momentum L. An explicit expression for this function is derived within the random-phase approximation using standard many-body techniques based on the Green's function method. Numerical results are presented for the wave-number dispersion and damping of the π-plasmon modes with different L's, demonstrating a unified picture of the π-plasmon-energy variation with q for the BN-DWNTs of different diameters. According to this picture, the spectrum of the π plasmons, which are shown to be long lived and hence well-defined collective electronic excitations in the BN-DWNTs, consists of a set of nonintersecting upward-dispersed branches, which are well separated in their energies at small values of q, but which tend to merge with increasing q. Each of the branches corresponds to one and only one value of the angular momentum $L=0,1,2,\ldots$ and none of the branches starts from $q=0$. The present calculations also show that the π plasmons in the BN-DWNTs can exist even at those q values at which the π-plasmon modes are not supported by either of the nanotube shells alone. It is found that the threshold value of the wavelength, at which the $L=0$ π-plasmon dispersion curve in the BN-DWNTs makes its start, is redshifted as compared to that in the inner and outer nanotube shells if they are considered separately. The most important features of our calculated results seem to be consistent, more or less reasonable, with those derived from the recent electron-energy-loss-spectroscopy experiment of Fuentes *et al.* [Phys. Rev. B **67**, 035429 (2003)] on a macroscopic assembly of BN multiwalled nanotubes of different diameters and chiralities, thus suggesting a universality of the properties of π plasmons in double-walled and multiwalled BN nanotubes.

DOI: 10.1103/PhysRevB.78.035415 PACS number(s): 73.22.−f, 73.20.−r, 79.20.Uv

I. INTRODUCTION

Initiated by the pioneering work of Rubio *et al.*[1] in 1994, boron nitride nanotubes (BN-NTs) have been the subject of intense theoretical and experimental investigations during the past decade. In particular, there have been a few research work devoted to the study of BN-NTs by means of high-resolution electron-energy-loss spectroscopy (EELS).[2–6] These EELS experiments have been carried out on both BN multiwalled nanotubes (BN-MWNTs) (Refs. 2–6) and BN single-walled nanotubes (BN-SWNTs).[6] For the latter ones, we have recently developed a theory that allows one to treat collective π-electronic excitations,[7] which are directly probed by EELS. The theory given in Ref. 7 is based on the well-known Ehrenreich-Cohen self-consistent-field approach[8] and explicitly takes into account the electronic band structure of the nanotubes, which we have calculated within a two-band tight-binding model using the zone-folding approximation, generalizing previous calculations performed for single-walled carbon nanotubes (CNTs).[9] The model employed in Ref. 7, though rather approximate, has the advantage of being conceptually and mathematically simple, enabling the basic properties of the collective plasmon modes in BN-SWNTs to be easily analyzed. We are unaware, however, of any theoretical studies of such properties relevant to BN-MWNTs. Meanwhile, at present there exist experimental data regarding those properties, obtained by Fuentes *et al.*[5] using momentum-resolved EELS. In the low-loss region (from 2 to 14 eV), the spectra measured in Ref. 5 exhibit a pronounced peak structure, which clearly results from excitation of π-plasmon modes. The position of the energy-loss peak was found to be shifted from 7.7 to 9.3 eV with increasing momentum transfer q from 0.1 to 0.6 Å^{-1}, thus suggesting a rather strong spatial dispersion of the π-plasmon modes excited in the experiment.

At this point we should emphasize that, although the essential physics involved in the problem under discussion is generally quite clear, a full theoretical analysis of the experimental data obtained in Ref. 5 is still lacking. A difficulty associated with this task is that the experiment[5] has been performed on a macroscopic assembly of BN-MWNTs of different diameters and chiralities, which have not, however, been characterized individually. Besides, the area probed by the primary electron beam was as large as 1 mm^2 so that an average signal from a great number of the nanotubes was measured in the experiment. As to the isolated BN-MWNTs, to the best of our knowledge, no momentum-resolved EELS experiments on such tubes have been carried out so far. Therefore, it may be worthwhile to present theoretical information on the properties of collective electronic excitations in individual BN-MWNTs, which might turn out to be useful as a guideline for future experimental studies. It should be noted, however, that, though it is in principle possible to

develop a corresponding theory for BN-MWNTs containing an arbitrary number of coaxial tubules (or shells), such a theory would inevitably be rather complicated, and, as a result, the underlying physics of the problem might be somewhat hidden. Therefore, as a first step toward a full theory, it seems to be reasonable to consider a simple special case, enabling a more transparent analytic treatment to be developed. Following this line, we focus our attention here on the simplest BN-MWNTs realization—namely, on BN double-walled nanotubes (BN-DWNTs). Note that a direct synthesis of such tubes is now available using arc-discharge techniques[10] (for a brief review of the subject, see, e.g., Ref. 11).

It is the main objective of the present paper to provide what we believe to be the first theoretical treatment of the collective π-electronic excitations in individual BN-DWNTs. The approach we are developing here is based on a standard field-theoretical formalism,[12,13] which is best suited for treating collective excitations of many-particle systems. All the calculations are carried out within the framework of the well-known Bohm-Pines random-phase approximation (RPA).[14] The formalism allows the effective dynamic-dielectric-response function of BN-DWNTs to be introduced in a natural way, and an explicit analytic expression, derived for this function, is then used to find the wave-number dispersion and damping of the π-plasmon modes in those systems by numerical means. Based on our calculations we conclude that a BN-DWNT can support the collective π-electronic excitations even at those values of the wave number q at which the π-plasmon modes do not exist in either of the shells (inner and outer) of the nanotube if they are taken separately. We also find that our theoretical results for the π-plasmon dispersion in BN-DWNTs appear to account satisfactorily for its main features observed in the experiment of Fuentes *et al.*,[5] thus suggesting that our findings are relevant not only to individual BN-DWNTs, which we are concerned with here, but, to some extent, to an assembly of BN-MWNTs as well. The reasons for such a rather surprising (but not quite unexpected) result, indicating a universality of the properties of π plasmons in double-walled and multiwalled BN nanotubes, deserve attention to be paid to and will be discussed further below.

The rest of the paper is arranged as follows. In Sec. II, we first formulate the model we use and present the formalism that forms the basis of the model calculations of the π-plasmon dispersion in BN-DWNTs. The results of those calculations and their discussion are given in Sec. III. In that section, our theoretical π-plasmon dispersion curves are also compared with the experimental data of Fuentes *et al.*[5] Finally, we give a summary of our main conclusions in Sec. IV.

II. MODEL AND THEORETICAL FORMALISM

In order to describe the collective electronic excitations in an individual BN-DWNT consisting of two coaxial BN-SWNTs, some knowledge of the geometrical structure of the latter is necessary. The geometry of BN-SWNTs is conventionally specified by the integer-valued dual index (l_1,l_2), which characterizes the way of rolling up a two-dimensional hexagonal BN sheet to form a cylinder. In terms of this pair of integers, the nanotube circumference vector $\mathbf{C}$ is defined as

$$\mathbf{C} = l_1\mathbf{a}_1 + l_2\mathbf{a}_2, \tag{1}$$

where $\mathbf{a}_1$ and $\mathbf{a}_2$ are the primitive lattice translation vectors of the above-mentioned BN sheet, making an angle of 120° and having the length equal to the lattice constant $a_0=\sqrt{3}d$ (where $d=1.45$ Å is the length of the B-N bond). With the preceding notation, the indices $(l,0)$, $(2l,l)$, and (l_1,l_2) with $l_1\neq l_2>0$ correspond (in sequential order) to zigzag, armchair, and chiral BN-SWNTs. It was reported that BN-SWNTs, synthesized by means of different techniques,[2,15,16] exhibit a chirality preference in having a zigzag structure. The situation is, however, much less clear for BN-DWNTs. In particular, to the best of our knowledge, no study has been reported so far on the chiral indices of two shells (inner and outer) of such tubes fabricated by using a plasma-arc method,[10] which yields macroscopic amounts of pure BN-DWNTs. Obviously, further experimental investigations are required to clarify this issue. On the other hand, theoretical band-structure calculations[17–21] predict that, unlike CNTs, all BN-NTs are semiconductors with a nearly constant band-gap energy of about 5.5 eV (except possibly the thinnest stable nanotubes, which can have a smaller band gap), independent of their radius and helicity and of whether the nanotubes are single-walled or multiwalled. It seems therefore reasonable to assume that representative results for characteristics of the collective electronic excitations in BN-DWNTs can be obtained by considering the simplest possible model in which two coaxial zigzag BN-SWNTs with the chiral indices $(l_1,0)$ and $(l_2,0)$ form a BN-DWNT $(l_1,0)@(l_2,0)$ with the innermost radius $R_1=l_1a_0/2\pi$ and the outermost radius $R_2=l_2a_0/2\pi$. In what follows, we focus our attention on just this system, shown schematically in Fig. 1. Generalization, if needed, to BN-DWNTs composed of coaxial tubule pairs with another helical structure is straightforward within the scheme we develop here, but it is beyond the scope of the present paper. Certainly, without a detailed theoretical analysis, one can only speculate about the effect of chirality on the basic properties of plasmons in BN-DWNTs. However, we guess its impact is minor. The reason for this is that the intertube electron transfer in BN-DWNTs is negligible (see further below) so that the plasmon behavior in those tubes should be affected mainly by the electronic structure of the constituent BN-SWNTs, which was shown to be actually independent of their chirality.[17–21]

To conclude the specification of the model just described, it should be noted that the distance between the inner shell and the outer one in BN-DWNTs is estimated to be equal to approximately 3.6 Å.[10] Because of this relatively large separation, which is much larger than the distance between nearest-neighboring atoms in each of the shells, the intershell electron transfer is expected to be small and can be safely ignored in treating the collective π-electronic modes (π plasmons) in those tubes since it can scarcely generate qualitatively new physics in the energy scale ($\sim$7–10 eV) typical of the π plasmons. In this energy range, no drastic modifi-

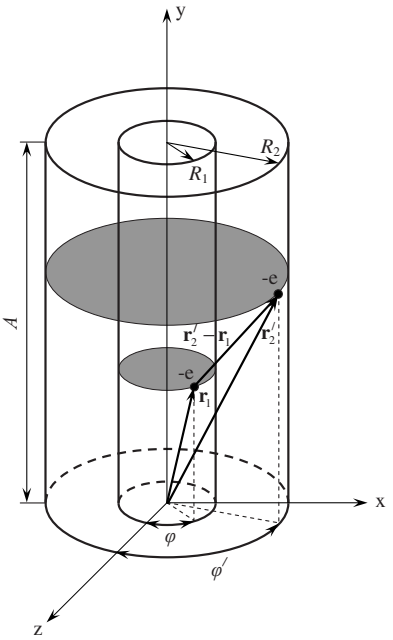

FIG. 1. Schematic illustration of the BN-DWNT with length A, the innermost radius R_1, and the outermost radius R_2. The vectors $\mathbf{r}_1$ and $\mathbf{r}_2'$ specify the positions of two π electrons (marked with heavy dots) localized on shells 1 and 2 of the nanotube, respectively. The angles φ and φ' of the cylindrical coordinate system are also shown.

cation of the π-band electronic structure of the tubes can also be expected on account of the weak van der Waals interaction between the atoms of one shell and those of the other in the same tubule. It follows from the above considerations that in the problem at hand, both the shells can be viewed as being coupled with one another only via long-range Coulomb interaction between the π electrons, which keep in their original shells after two-particle scattering events. An interesting question that arises here is how this interaction manifests itself in the properties of the π-plasmon excitations supported by the whole double-walled tubule system under consideration; in particular, one may inquire if their characteristics are distinctly different from those of π plasmons in either of the constituent BN-SWNTs. Our results, which will be presented in detail below, show that the answer is clearly affirmative.

These details can be quantified by developing a systematic and analytic approach, which would allow us to characterize the π plasmons in the BN-DWNTs $(l_1,0)@(l_2,0)$ in terms of the band-structure parameters of the constituent zigzag BN-SWNTs. With this end in view, it seems to be appropriate to rely on an analytic model of the electronic structure of the BN-SWNTs, developed in our previous paper[7] on the basis of the nearest-neighboring tight-binding approximation by using the zone-folding method. Details of the model are given in Ref. 7 and need not be repeated here. In this paper, we present only the main outcome of the model—namely, the expression for the π-electron-energy dispersion in a BN-SWNT $(l,0)$, which is given by

$$E_{m\pm}(k) = \pm \left\{ \Delta^2 + t_0^2 \left[1 + 4\cos^2\left(\frac{\pi m}{l}\right) + 4\cos\left(\frac{\pi m}{l}\right)\cos\left(\frac{3kd}{2}\right) \right] \right\}^{1/2}. \tag{2}$$

Hereafter the upper (lower) sign refers to the conduction (valence) band, $m=0,\pm 1,\pm 2,\ \ldots,\pm(l-1)$ is the azimuthal quantum number labeling the size-quantized energy subbands, and k is the one-dimensional wave vector along the tube axis, which takes values within the one-dimensional Brillouin zone of the nanotube, i.e., $k\in[-k_{\mathrm{BZ}},k_{\mathrm{BZ}}]$, where $k_{\mathrm{BZ}}=\pi/3d$. The energy π bands of Eq. (2) are parametrized by the difference 2Δ of energies of π electrons localized on the B and N sites and by the transfer integral t_0 between π orbitals of nearest-neighboring B and N atoms.

Following Ref. 7, the periodic part of the Bloch function for those bands can be approximately expressed as

$$u_{mk\pm}(\mathbf{r}) = C^{(1)}_{mk\pm}U^{(1)}_{\mathbf{K}}(\mathbf{r}) + C^{(2)}_{mk\pm}U^{(2)}_{\mathbf{K}}(\mathbf{r}), \tag{3}$$

where the superscripts 1 and 2 denote the two sublattices occupied by B and N atoms, respectively,

$$C^{(1)}_{mk\pm} = -\frac{t_0[e^{ikd}+2\cos(\pi m/l)e^{-ikd}]}{\sqrt{2E_{m+}(k)[E_{m+}(k)\mp\Delta]}}, \tag{4}$$

$$C^{(2)}_{mk\pm} = \pm\sqrt{\frac{E_{m+}(k)\mp\Delta}{2E_{m+}(k)}}, \tag{5}$$

$$U^{(1)}_{\mathbf{K}}(\mathbf{r}) = \frac{1}{\sqrt{N}}\sum_n \phi(\mathbf{r}-\mathbf{R}_n)\exp\{-i\mathbf{K}(\mathbf{r}-\mathbf{R}_n)\}, \tag{6}$$

$$U^{(2)}_{\mathbf{K}}(\mathbf{r}) = \frac{1}{\sqrt{N}}\sum_n \phi(\mathbf{r}-\mathbf{R}_n-\mathbf{d})\exp\{-i\mathbf{K}(\mathbf{r}-\mathbf{R}_n-\mathbf{d})\}. \tag{7}$$

Here $\mathbf{K}=(2\pi/3d)(1/\sqrt{3},1)$ is the wave vector for the K point of the two-dimensional hexagonal Brillouin zone of the BN sheet, $\mathbf{R}_n$ stands for the position vector of the nth unit cell, $\mathbf{d}$ denotes the vector connecting the two atoms within a unit cell, $\phi(\mathbf{r}-\mathbf{R}_n)$ is the wave function of a normalized π orbital for an atom located at $\mathbf{R}_n$, and N is the total number of the sites occupied by B and N atoms, which is given by

$$N = \frac{4Al}{3d}, \tag{8}$$

where A is the normalized length of the nanotube. Note that the zone-folding-derived π-electronic states of the zigzag BN-SWNTs [Eq. (3)] are double valley-degenerate due to the presence of the states associated with the valley centered at the K' point [with the wave vector $\mathbf{K}'=(2\pi/3d)(2/\sqrt{3},0)$] of the original Brillouin zone of the BN sheet.

We next turn to the description of the Coulomb interaction among the π electrons of a BN-DWNT in the geometry illustrated in Fig. 1. As we remarked earlier, without electron tunneling between two shells of the nanotube, only the two-particle scattering processes, in which the electrons keep

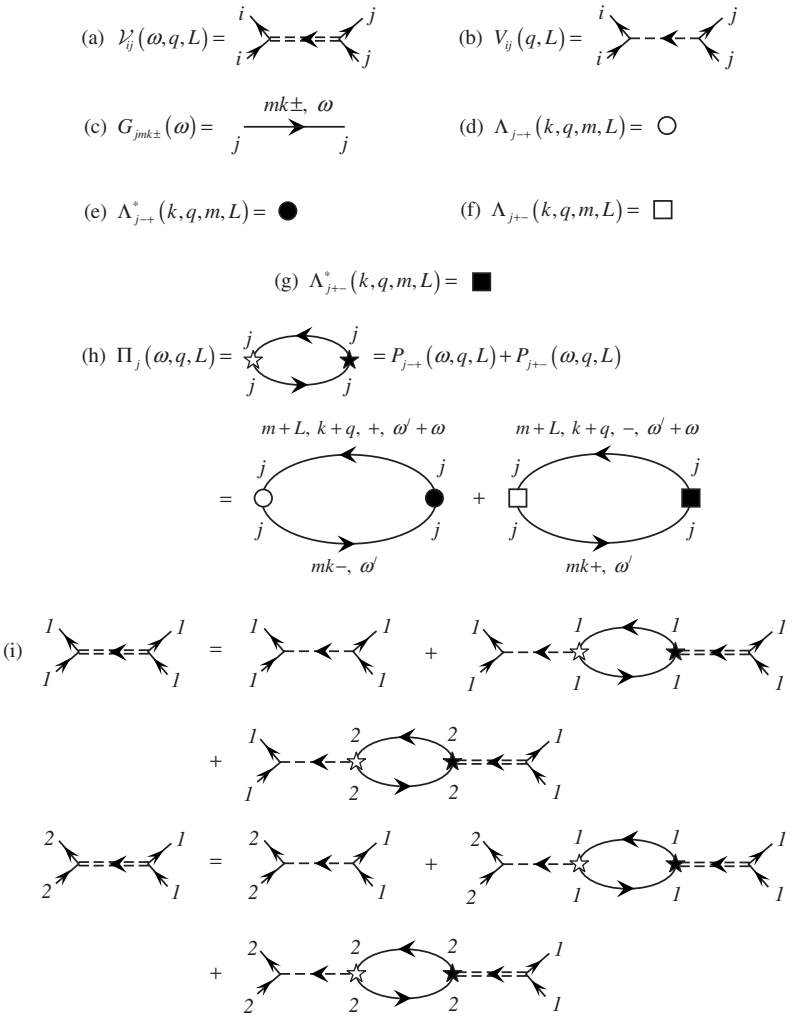

FIG. 2. (a)–(h) define the basic graphical vocabulary, i.e., the Feynman diagrams representing the basic quantities $\mathcal{V}_{ij}$, V_{ij}, $G_{jmk\pm}$, $\Lambda_{j-+(+-)}$, $\Lambda^{*}_{j-+(+-)}$, and Π_j of the problem. The indices i and j denote the shells of the nanotube, $\mathcal{V}_{ij}$ is the effective screened interaction, V_{ij} is the "bare" Coulomb interaction, $G_{jmk\pm}$ is the Green's function of the noninteracting π electrons, $\Lambda_{j-+(+-)}$ and $\Lambda^{*}_{j-+(+-)}$ are the vertices at which Coulomb lines join fermion lines, and Π_j is a generalized irreducible interband polarization function. (i) Diagrammatic representation of a pair of coupled equations for the effective interactions $\mathcal{V}_{11}$ and $\mathcal{V}_{21}$ in the RPA.

in their original shells, should be taken into account. Since each of the shells possesses translational symmetry along the tubule axis and rotational symmetry around it, the transferred momentum q and the angular momentum $L=0,\pm1,\pm2,\ \ldots$ corresponding to those symmetries must be conserved in the process of the scattering. It is therefore advantageous to introduce a Fourier representation of the Coulomb interaction in the variables q and L. In the cylindrical coordinates (R,φ,y) shown in Fig. 1, the Fourier-series expansion of the Coulomb potential $V(\mathbf{r}_i-\mathbf{r}'_j)$ between two electrons at point $\mathbf{r}_i$ and $\mathbf{r}'_j$ is given by

$$V(\mathbf{r}_i-\mathbf{r}'_j)=\sum_{L=-\infty}^{\infty}\sum_{q}V_{ij}(q,L)e^{iL(\varphi-\varphi')}e^{iq(y-y')},\qquad(9)$$

with the associated Fourier coefficients

$$V_{ij}(q,L)=\frac{2e^2}{\varepsilon_b A}[\delta_{ij}I_L(qR_i)K_L(qR_i)+(1-\delta_{ij})I_L(qR_1)K_L(qR_2)],\quad R_1<R_2,\qquad(10)$$

where the two subscripts $i=1,2$ and $j=1,2$ label the shells of the nanotube, ε_b is a background dielectric constant describing the screening effect of the interaction due to the polarization of core electrons, δ_{ij} is the Kronecker delta symbol, and $I_L(qR_i)$ and $K_L(qR_i)$ are the Lth-order modified Bessel functions of the first and second kinds, respectively.

Due to the symmetry properties mentioned above, the collective π-electronic modes of the system under consideration may also be specified by the angular-momentum quantum number L and the component of the wave vector q along the tube axis. The frequencies $\omega_L(q)$ of those modes can be calculated by using standard many-body techniques based on the Green's function method.[12,13] Within this field-theoretical approach, the π-plasmon frequencies are defined as poles of the effective screened Coulomb interaction $\mathcal{V}_{ij}$ between the π electrons, which depends only on ω, q, and L. To obtain the basic equation that serves for determining the poles, it is sufficient to consider two functions $\mathcal{V}_{11}(\omega,q,L)$ and $\mathcal{V}_{21}(\omega,q,L)$. Within the RPA, both the functions can be obtained by solving a pair of the coupled algebraic equations shown diagrammatically in Fig. 2(i),

$$\mathcal{V}_{11}(\omega,q,L)=V_{11}(q,L)+V_{11}(q,L)\Pi_1(\omega,q,L)\mathcal{V}_{11}(\omega,q,L)+V_{12}(q,L)\Pi_2(\omega,q,L)\mathcal{V}_{21}(\omega,q,L),\qquad(11)$$

$$\mathcal{V}_{21}(\omega,q,L)=V_{21}(q,L)+V_{21}(q,L)\Pi_1(\omega,q,L)\mathcal{V}_{11}(\omega,q,L)+V_{22}(q,L)\Pi_2(\omega,q,L)\mathcal{V}_{21}(\omega,q,L).\qquad(12)$$

Here $\Pi_j(\omega,q,L)$ is a generalized interband polarization function represented by "bubble" diagram (h) in Fig. 2 and involving two terms,

$$\Pi_j(\omega,q,L) = P_{j-+}(\omega,q,L) + P_{j+-}(\omega,q,L), \tag{13}$$

with

$$P_{j-+}(\omega,q,L) = \sum_{m=-(l_j-1)}^{l_j-1} 4A \int_{-k_{\mathrm{BZ}}}^{k_{\mathrm{BZ}}} \frac{dk}{2\pi} |\Lambda_{j-+}(k,q,m,L)|^2 i \times \int \frac{d\omega'}{2\pi} G_{jm+L,k+q+}(\omega'+\omega) G_{jmk-}(\omega'), \tag{14}$$

and with $P_{j+-}(\omega,q,L)$ of the same form as in Eq. (14), but with the subscript + replaced by − and vice versa. The factor 4 in front of the integral over k in the above equation is due to the spin and the valley degeneracies of the π-electronic states in each of the nanotube shells (for details, see Ref. 7). The two other quantities entering Eq. (14) are the vertex function $\Lambda_{j-+}(k,q,m,L)$ [diagram (d) in Fig. 2] and the Green's function $G_{jmk\pm}(\omega)$ of the noninteracting π electrons [diagram (c) in Fig. 2]. The former is defined as the following matrix element for the transitions between the valence band and the conduction one,

$$\Lambda_{j-+}(k,q,m,L) = \int u^*_{mk-}(\mathbf{r}) u_{m+L,k+q+}(\mathbf{r}) d\mathbf{r}, \tag{15}$$

where the integration extends over a unit cell. Similarly, we define the interaction vertex $\Lambda_{j+-}(k,q,m,L)$, represented by diagram (f) in Fig. 2, as the above expression with the subscripts + and − interchanged. As to the Green's function $G_{jmk\pm}(\omega)$, it can be written in a standard form with the assumption of no importance of temperature effects,

$$G_{jmk\pm}(\omega) = [\hbar\omega - E_{jm\pm}(k) + i\delta \cdot \mathrm{sign}\ \omega]^{-1}, \tag{16}$$

where $\delta \to 0$.

With the definition of the vertex function given above and using Eqs. (3)–(8), it can be easily shown that the vertex factor $|\Lambda_{j-+}|^2$ in Eq. (14) is expressed as

$$|\Lambda_{j-+}(k,q,m,L)|^2 = |\Lambda_{j+-}(k,q,m,L)|^2 = \frac{1}{2}\left[1 - \frac{\Delta^2 + t_0^2 F_j(k,q,m,L)}{E_{jm+}(k) E_{jm+L+}(k+q)}\right], \tag{17}$$

with

$$F_j(k,q,m,L) = \cos(qd) + 4\cos\left(\frac{\pi m}{l_j}\right)\cos\left[\frac{\pi(m+L)}{l_j}\right] \times \cos\left(\frac{qd}{2}\right) + 2\cos\left(\frac{\pi m}{l_j}\right)\cos\left[\left(\frac{3}{2}k+q\right)d\right] + 2\cos\left[\frac{\pi(m+L)}{l_j}\right]\cos\left[(3k+q)\frac{d}{2}\right]. \tag{18}$$

Using the Green's function, defined by Eq. (16), to evaluate the integral over ω' in Eq. (14), we arrive at the following expression for the "fermion loop" in the standard zero-temperature-diagram technique,[12,13]

$$i\int \frac{d\omega'}{2\pi} G_{jm+L,k+q+}(\omega'+\omega) G_{jmk-}(\omega') = \frac{-1}{E_{jm+L+}(k+q) - E_{jm-}(k) - \hbar\omega - i\hbar\Gamma}. \tag{19}$$

In obtaining this formula, we have replaced the infinitesimal positive δ by a phenomenological level broadening parameter Γ in order to take into account the fact that in real physical systems of interest there always exist single-particle scattering processes having a smoothing effect on the singularity inherent in Eq. (19) in the limit $\Gamma \to 0$.

Before going back to Eqs. (11) and (12), it is worth noticing that neither the summation over m nor the integration over k in Eq. (14) can be performed analytically because of the complexity of both the π-electron-energy dispersion [Eq. (2)] and the whole integrand in Eq. (14). However, with the explicit expressions obtained above [Eqs. (17)–(19)], the remaining summation and integration in Eq. (14) are easy to implement by numerical means, and this is the way that we will follow further below in our theoretical study (see Sec. III).

If we restrict our attention to π-plasmon energies, we have to find the poles of $\mathcal{V}_{21}$ or, which is the same, $\mathcal{V}_{11}$, i.e., the solutions of the following equation, which represent the condition for the pair of the linear inhomogenous Eqs. (11) and (12) to have a null secular determinant,

$$[1 - V_{11}(q,L)\Pi_1(\omega,q,L)][1 - V_{22}(q,L)\Pi_2(\omega,q,L)] - V_{12}^2(q,L)\Pi_1(\omega,q,L)\Pi_2(\omega,q,L) = 0. \tag{20}$$

As is well known, the self-sustaining collective modes of an interacting electron system can be identified with the zeros of the dynamic-dielectric-response function $\varepsilon(\omega,q)$ of the system.[14] This allows us to interpret the left-hand side of Eq. (20) as an effective dynamic-dielectric-response function $\varepsilon_{\mathrm{eff}}(\omega,q,L)$ of the composite system of the two tubules, which we are concerned with here. The "dressed" Coulomb interaction $\mathcal{V}_{21}$ is then given by

$$\mathcal{V}_{21}(q,L) = \frac{V_{21}(q,L)}{\varepsilon_{\mathrm{eff}}(\omega,q,L)}, \tag{21}$$

defining an analytical framework for treating collective excitations in BN-DWNTs. To avoid ambiguity, one comment is in place with regard to this equation. The $\varepsilon_{\mathrm{eff}}$, defined in such a way, by itself is not a physically relevant quantity if we would like to use it to determine the electron-energy-loss function $S(\omega,q) = -\mathrm{Im}[1/\varepsilon(\omega,q)]$ since it does not, in general, meet the usual analyticity requirements[22] (in particular, its imaginary part is not always positive over the whole frequency region $\omega > 0$, which might give rise to false "negative electron-energy-losses"). It is evident, therefore, that the $\varepsilon_{\mathrm{eff}}$ introduced above is merely a convenient abbreviation notation of the left-hand side of Eq. (20) and does not make any sense beyond the problem at hand. On the contrary, the expressions within the first and the second square brackets in Eq. (20) have a clear physical meaning. Indeed, up to the factor ε_b, they represent, respectively, the true dynamic-dielectric-response functions $\varepsilon_1(\omega,q,L)$ and $\varepsilon_2(\omega,q,L)$ of

the two constituent BN-SWNTs if the latter are considered separately, i.e., if the Coulomb coupling between them is neglected. The dynamic-dielectric response of such tubes, determined by the dielectric function

$$\varepsilon_j(\omega,q,L) = \varepsilon_b[1 - V_{jj}(q,L)\Pi_j(\omega,q,L)] \tag{22}$$

in the RPA, was studied in detail in Ref. 7, providing insight into the physical nature of the collective excitations in BN-SWNTs. This gives us confidence that the heuristic approach, based on the above-mentioned dielectric function ε_{eff} of Eq. (21), has to be suffice to provide benchmark results for dispersion and damping of π plasmons in the case of BN-DWNTs. To facilitate a comparison with the results obtained in Ref. 7, it is convenient to express the ε_{eff} in terms of the above-mentioned dielectric functions ε_1 and ε_2. Using Eqs. (20) and (22), it is easy to show that the real and imaginary parts of ε_{eff} are given by

$$\begin{aligned}\text{Re}\ \varepsilon_{\text{eff}}(\omega,q,L) = \{&V_{12}^2(q,L)\varepsilon_b[\text{Re}\ \varepsilon_1(\omega,q,L) + \text{Re}\ \varepsilon_2(\omega,q,L) \\ &- \varepsilon_b] + [V_{11}(q,L)V_{22}(q,L) - V_{12}^2(q,L)] \\ &\times\ [\text{Re}\ \varepsilon_1(\omega,q,L)\text{Re}\ \varepsilon_2(\omega,q,L) \\ &- \text{Im}\ \varepsilon_1(\omega,q,L)\text{Im}\ \varepsilon_2(\omega,q,L)]\} \\ &\times[\varepsilon_b^2 V_{11}(q,L)V_{22}(q,L)]^{-1},\end{aligned} \tag{23}$$

$$\begin{aligned}\text{Im}\ \varepsilon_{\text{eff}}(\omega,q,L) = \{&V_{12}^2(q,L)\varepsilon_b[\text{Im}\ \varepsilon_1(\omega,q,L) + \text{Im}\ \varepsilon_2(\omega,q,L)] \\ &+ [V_{11}(q,L)V_{22}(q,L) - V_{12}^2(q,L)] \\ &\times\ [\text{Re}\ \varepsilon_1(\omega,q,L)\text{Im}\ \varepsilon_2(\omega,q,L) \\ &- \text{Re}\ \varepsilon_2(\omega,q,L)\text{Im}\ \varepsilon_1(\omega,q,L)]\} \\ &\times[\varepsilon_b^2 V_{11}(q,L)V_{22}(q,L)]^{-1}.\end{aligned} \tag{24}$$

The π-plasmon frequencies $\omega_L(q)$ can finally be determined as the solutions $\omega=\omega_L(q)$ of the equation

$$\text{Re}\ \varepsilon_{\text{eff}}(\omega,q,L) = 0. \tag{25}$$

If simultaneously Im $\varepsilon_{\text{eff}}(\omega,q,L)$ vanishes at those frequencies, the π-plasmon modes are undamped. As we shall see further below (Sec. III), this is not the case for the system under consideration, and the lifetime $\gamma_L(q)$ of the modes is finite so that the solution of Eq. (25) in the complex ω plane is $\omega=\omega_L(q)-i\gamma_L(q)$. The condition for such modes to be long-lived and hence well-defined collective excitations of the system requires the following inequality to be satisfied:

$$\frac{\gamma_L(q)}{\omega_L(q)} \ll 1. \tag{26}$$

For frequencies in the near vicinity of $\omega_L(q)$, the imaginary part of the solution can be approximated as

$$\gamma_L(q) = \left.\frac{\text{Im}\ \varepsilon_{\text{eff}}(\omega,q,L)}{\frac{\partial}{\partial\omega}\text{Re}\ \varepsilon_{\text{eff}}(\omega,q,L)}\right|_{\omega=\omega_L(q)}, \tag{27}$$

which must be positive if the dielectric response we are considering is causal. The above Eqs. (26) and (27) suggest a simple way to check whether a zero of the real part of ε_{eff} does correspond to a weakly damped collective mode—namely, one must first check the signs of Im ε_{eff} and ∂ Re $\varepsilon_{\text{eff}}/\partial\omega$, which should be positive at $\omega=\omega_L(q)$, and then to check the fulfilment of the condition of Eq. (26). Thus, the wave-number dispersion and damping of the π-plasmon modes may be deduced from the scans of the real and imaginary parts of ε_{eff} as functions of the frequency ω at different values of q and L. It is in this manner that both the characteristics of the π plasmons will be studied in Sec. III.

Before concluding this section, we would like to comment on some of the approximations, on which the theory developed above is based, and to emphasize the limitations arising from them. The most essential approximation used in our theory is the RPA ("the bubble-diagram approximation"). Whether the RPA is valid for the description of the dielectric response of the systems, which we are interested in here, remains an open question. Clearly, a complete theoretical analysis of the dielectric response, going beyond the RPA and including exchange-correlation effects, is needed to arrive at a definite conclusion on this point. Unfortunately, at present we do not know how to formulate such a theory in a systematic and analytically tractable manner. However, we do not expect that the corrections due to the exchange-correlation effects will be qualitatively significant. At this point, we are encouraged by the recent *ab initio* density-functional-theory calculations of the optical properties of BN-SWNTs of very small radius, carried out by Park *et al.*[23] and Wirtz *et al.*[24] These calculations show that in the optical (long wavelength) limit ($q\to 0$) the quasiparticle self-energy corrections are almost compensated by the effects of electron-hole attraction (excitonic effects). Thus, the many-particle corrections on the whole have a minor net effect, and hence the RPA-plasmon results can be trusted, at least at a qualitative level. Within the RPA plus the local-density approximation, it has previously been shown[25] that the local-field effects have no significant influence on the loss spectra of the above-mentioned nanotubes if the transferred momentum $q\to 0$ is directed along the tube axis. Recently, Perez and Que[26] arrived at the same conclusion in the case of single-walled CNTs of fairly large diameters (more than 1.4 nm). We believe that it is reasonable to speculate on the validity of this conclusion for BN-DWNTs as well.

One more essential limitation of our theory is that it is entirely based on the π-electron approximation. In consequence, the theory is unable to describe the high-frequency collective modes associated with both π and σ electrons (the so-called $\pi+\sigma$ plasmons). Meanwhile, a clear evidence of the excitation of such modes in BN-MWNTs has been obtained in the EELS experiment of Fuentes *et al.*,[5] where they manifest themselves as a pronounced high-energy peak structure in the loss spectra. An extension of the theory developed above to correctly include the σ electrons remains an open question for future theoretical work.

III. NUMERICAL RESULTS AND DISCUSSION

The material presented in this section deals with the application of the theory developed in Sec. II to a number of specific examples of BN-DWNTs. We consider three zigzag-type BN-DWNTs (17,0)@(25,0), (25,0)@(33,0), and

(37,0)@(45,0), focusing our attention mainly on the first of them since, as will become clear further, the results obtained for that tube are representative ones for all the other tubes of this type as well. The outer diameters of the three nanotubes, chosen for the investigation in this study, are, respectively, 1.99, 2.63, and 3.59 nm, covering, even with something to spare, the outer-diameter range of most currently synthesized BN-DWNTs.[10] It is also worth noting that the inner diameter ($\simeq$2.95 nm) of the BN-DWNT (37,0)@(45,0) is very close to the mean innermost diameter ($\simeq$3.1 nm) of the BN-MWNTs studied in the EELS experiment of Fuentes *et al.*[5]

The computation of the effective dynamic-dielectric-response function $\varepsilon_{\text{eff}}(\omega,q,L)$, according to Eqs. (23) and (24), requires a knowledge of the values of a number of parameters, which are the essential ingredients of the theory developed above. First, we need to choose the values of the π-electron band parameters Δ and t_0 entering Eq. (2). Ideally, both the parameters have to be brought into contact with actual EELS experiments relevant to BN-DWNTs. As remarked earlier, such experiments, which could provide enough information to make a proper choice of Δ and t_0 possible, are still missing at present. Under the circumstances, any particular choice of the parameters can hardly be made without some ambiguity. In what follows, we fix the parameter Δ at the value of 2.2 eV, which corresponds to that adopted in our previous papers.[7,27] This value lies in the range of the reported values of Δ, which were obtained by optical-absorption measurements,[28] as well as by a scanning tunneling spectroscopy study.[29] As to the parameter t_0, we will treat it as a freely adjustable parameter to give the best fit of our calculated results for the π-plasmon energies in the BN-DWNTs to those obtained experimentally for BN-MWNTs[5] (see Fig. 6 further below). Though beforehand it is not quite clear to what extent our theory is applicable to those nanotubes, it is still the best one can do at this stage. Following this line, we have performed a number of numerical simulations to estimate the proper value of t_0 and have found that the value $t_0=2$ eV, whose justification from first principles is clearly lacking, is the most appropriate one for the problem at hand.

One more parameter, relevant to our problem and occurring in Eq. (19), is the damping factor Γ, which regularizes, in a phenomenological way, the resonant divergencies of the polarization function $\Pi_j(\omega,q,L)$ in Eq. (13). We are not aware of any experimental data available at present, which would enable an unambiguous choice of the parameter Γ to be made. Therefore, in what follows, the $\hbar\Gamma$ value is taken, rather arbitrary, to be equal to 0.16 eV independent of the shell index j, the energy-subband quantum number m, and the wave vector k. Thus, the corresponding dimensionless broadening parameter $\hbar\Gamma/t_0=0.08$ is the same as that adopted in our previous paper,[7] where it was used to calculate the EELS spectra of BN-SWNTs and recognized as being rather realistic. Based on our model calculation in Ref. 27, as well as on the *ab initio* investigations in a recent paper by Guo *et al.*,[30] we adopt the value of 2.5 for the dielectric constant ε_b, describing the screening effect due to all excitations outside the π bands. It is this value that we use as an input in the calculation of the effective dielectric function $\varepsilon_{\text{eff}}(\omega,q,L)$ given by Eqs. (23) and (24).

In Fig. 3, we display the spectra of the real and imaginary parts of the $\varepsilon_{\text{eff}}(\omega,q,L)$, numerically calculated for the BN-DWNT (17,0)@(25,0) at a fixed value of the wave number q (equal to $0.3k_{\text{BZ}}$ in this case). Two different values of L, namely, $L=0$ and $L=1$, have been taken in order to illustrate the effect of the angular momentum L on the calculated spectra. To stress the difference between the present results and those in Ref. 7, we have also plotted in Fig. 3 the curves of the real and imaginary parts of the true dynamic-dielectric-response functions $\varepsilon_{1,2}(\omega,q,L)$ of the two constituent BN-SWNTs (17,0) and (25,0), which have been calculated using Eq. (22).

As mentioned in Sec. II, the π-plasmon frequency $\omega_L(q)$ is obtained as a solution of Eq. (25), involving only the real part of $\varepsilon_{\text{eff}}(\omega,q,L)$, with an additional restriction imposed by the inequality of Eq. (26), which, according to Eq. (27), involves also the imaginary part of $\varepsilon_{\text{eff}}(\omega,q,L)$. Figure 3 permits one to find the corresponding solution by scanning the graphs of the real and imaginary parts of $\varepsilon_{\text{eff}}(\omega,q,L)$. As seen from Figs. 3(a) and 3(c), the graph of Re $\varepsilon_{\text{eff}}(\omega,q,L)$ passes through zero two times. It is evident that the zero at the lower frequency, marked with an open circle in Figs. 3(a) and 3(c), does not correspond to a collective mode at all because the sign of the denominator in Eq. (27) is negative at that frequency. Besides this, as seen from Figs. 3(b) and 3(d), at that point the imaginary part of $\varepsilon_{\text{eff}}(\omega,q,L)$ is not at all small so that the inequality of Eq. (26) cannot be fulfilled in any case. On the contrary, the higher-frequency zero, marked with a solid circle in Figs. 3(a) and 3(c), may apparently be recognized as corresponding to a well-defined collective electronic excitations that can be supported by the system since from Figs. 3(b) and 3(d) we conclude that the imaginary part of $\varepsilon_{\text{eff}}(\omega,q,L)$ at that frequency is very small. This conclusion is confirmed by a more careful analysis of the ratio $\gamma_L(q)/\omega_L(q)$ conducted further below (see Table I), which shows how small the plasmon damping is.

One more result, following from Fig. 3, is noteworthy. Since we see that only a single "antiresonant" (dip) structure with the two zeros of Re $\varepsilon_{\text{eff}}(\omega,q,L)$ (one on the left side and one on the right side) is present in all the spectra shown in Figs. 3(a) and 3(c), one can conclude that there exists only one π-plasmon mode for each value of the angular momentum $L=0,1$ and the value of q given in Fig. 3. We have examined the other values of q, at which the π-plasmon modes exist, and always found only a single true π-plasmon mode for those L's. This important feature is, in fact, common to all the zigzag BN-DWNTs considered in this paper (see Fig. 4 further below). Note that a similar result of no multiple solutions to the equation $\varepsilon_j(\omega,q,L)=0$ has been obtained for zigzag BN-SWNTs in our previous paper,[7] where it was commented on more extensively.

From the comparison of the graphs in Figs. 3(a) and 3(c), we see that the zero of the function Re $\varepsilon_{\text{eff}}(\omega,q,L)$, corresponding to the π-plasmon mode in the BN-DWNT, suffers a pronounced shift to higher energies with increasing L. From those figures, we can also see that a behavior precisely the same as just mentioned above, but only less clearly visible, is inherent in the π-plasmon frequencies [i.e., in higher-frequency zeros of the functions Re $\varepsilon_{1,2}(\omega,q,L)$] of the constituent BN-SWNTs, a result we have pointed out earlier in

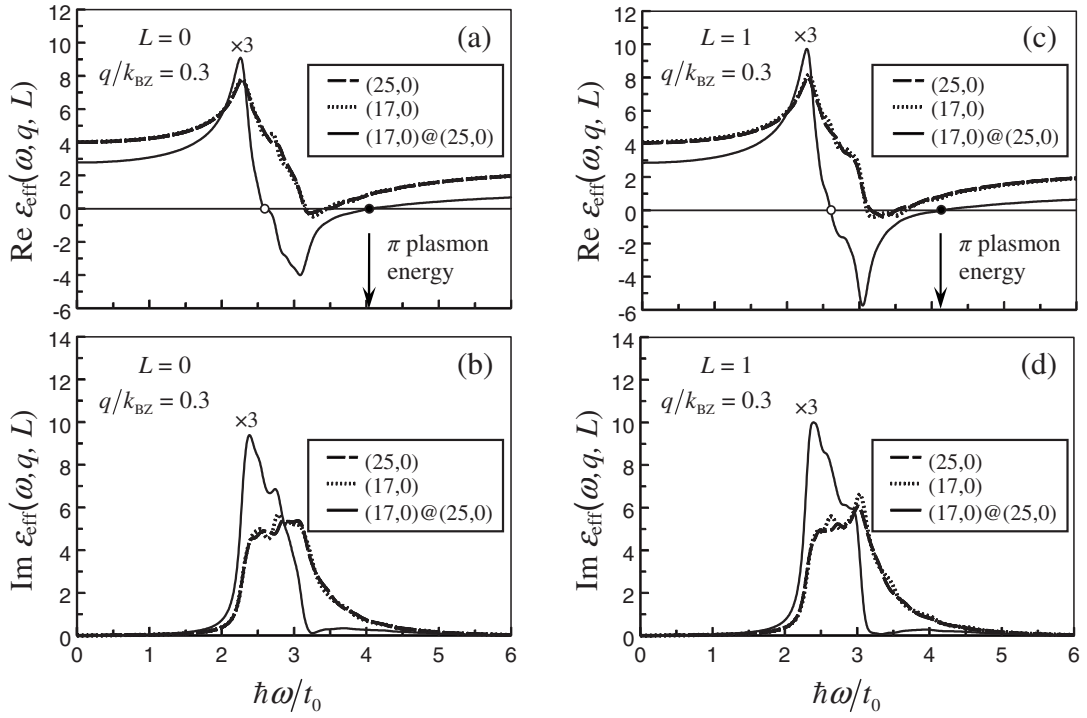

FIG. 3. The real and imaginary parts of the effective dynamic-dielectric-response function $\varepsilon_{\text{eff}}(\omega,q,L)$ are plotted versus $\hbar\omega/t_0$ for the BN-DWNT (17,0)@(25,0) (solid lines). For comparison the real and imaginary parts of the true dynamic-dielectric functions $\varepsilon_{1,2}(\omega,q,L)$ of the two constituent BN-SWNTs (17,0) (dotted lines) and (25,0) (dashed lines) are also shown. The results for the BN-DWNT and the BN-SWNTs are obtained using Eqs. (23) and (24) and Eq. (22), respectively. The value of the wave number q is fixed at $0.3k_{\text{BZ}}$; the angular momentum L is chosen to be 0 (left panels) and 1 (right panels). The other parameters used to generate this figure are given in the text. The sign $\times 3$ above the solid lines means that the values of the functions Re $\varepsilon_{\text{eff}}(\omega,q,L)$ and Im $\varepsilon_{\text{eff}}(\omega,q,L)$ are obtained from those in the figure by multiplying them by factor 3. The open and solid circles mark the zeros of Re $\varepsilon_{\text{eff}}(\omega,q,L)$. The arrow on the horizontal axis indicates the location of the π-plasmon energy.

Ref. 7, where it was attributed to an increase in the minimal energy required for the π electrons to be excited from the subbands dispersed upward in the valence band to those dispersed downward in the conduction band, as the angular momentum L increases. However, at this time we are unable to offer such a qualitative account of the blue shift of the π-plasmon energy with increasing L in the case of BN-DWNTs. The reason for this is that, as remarked in Sec. II, the response function $\varepsilon_{\text{eff}}(\omega,q,L)$, we deal with here, is not a true dielectric function of the BN-DWNTs, and hence the resonant and antiresonant structures, occurring in the spectra of $\varepsilon_{\text{eff}}(\omega,q,L)$, do not allow the intuitive interpretation to be given to them in terms of the single-particle interband transitions in the constituent BN-SWNTs. Besides, it should be stressed that in any case the collective nature of the π-plasmon modes we are considering implies that, in general, there is no direct correlation between the π-plasmon energies and those of the above-mentioned transitions. On the basis of our calculations, we can only state that the trend of the L π-plasmon energy to be the larger, the larger is the L value, is common to all the BN-DWNTs we have examined. However, the effect becomes negligible with increasing the wave number q so that at fairly large q values the dispersion curves of the π plasmons with different L's merge with one another, which is clearly in evidence in Fig. 6 further below.

TABLE I. The calculated values of the dimensionless damping factor $\gamma_L(q)/\omega_L(q)$ for the $L=0,1,2$ π-plasmon modes in the BN-DWNT (17,0)@(25,0) at several values of the dimensionless wave number q/k_{BZ}.

	$\gamma_L(q)/\omega_L(q)$		
q/k_{BZ}	$L=0$	$L=1$	$L=2$
0.15	0.140	0.100	0.072
0.20	0.124	0.093	0.087
0.30	0.084	0.062	0.057
0.40	0.063	0.085	0.066
0.50	0.049	0.053	0.051
0.60	0.043	0.048	0.039

In Fig. 4, we show the spectra of the real and imaginary parts of $\varepsilon_{\text{eff}}(\omega,q,L)$ for the three selected BN-DWNTs, calculated for the two different values of the angular momentum $L(=0,1)$ at the wave number $q=0.3k_{\text{BZ}}$. A remarkable fact, which follows from Figs. 4(a) and 4(c), is that the curves of Re $\varepsilon_{\text{eff}}(\omega,q,L)$ for the nanotubes (25,0)@(33,0) and (37,0)@(45,0) pass through zero at the same two points as the curve of Re $\varepsilon_{\text{eff}}(\omega,q,L)$ for the BN-DWNT (17,0)@(25,0). This, along with the overall smallness of Im $\varepsilon_{\text{eff}}(\omega,q,L)$ at the higher-frequency zero point of Re $\varepsilon_{\text{eff}}(\omega,q,L)$ for all the three nanotubes [see Figs. 4(b) and 4(d)], implies that the main characteristics of the π plasmons

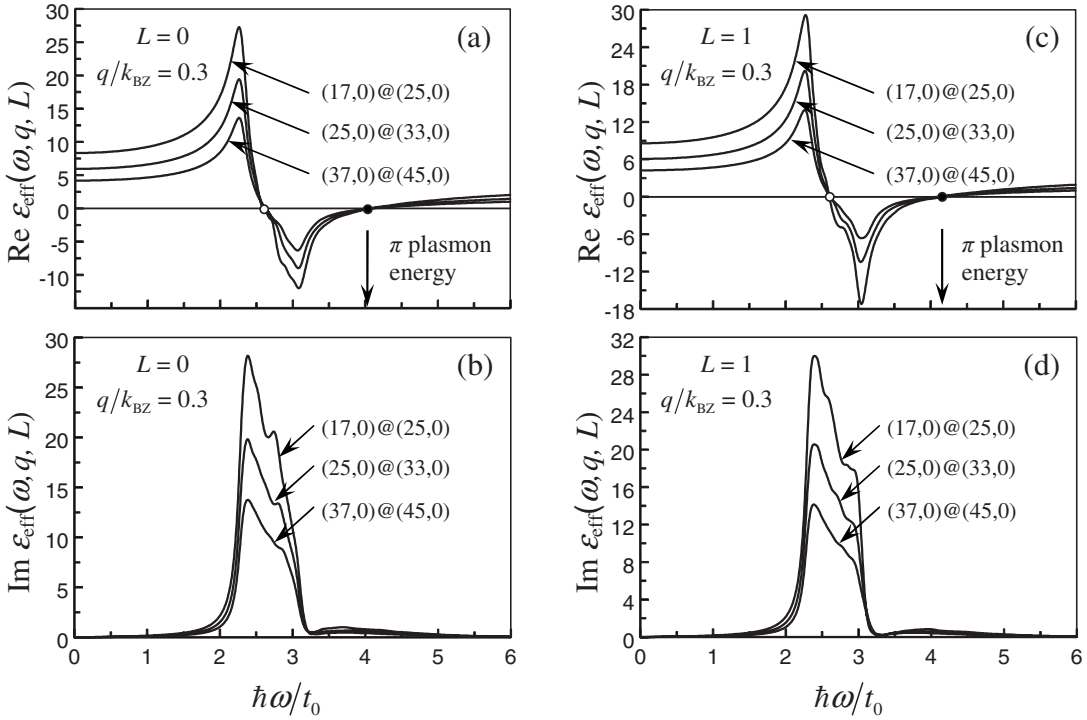

FIG. 4. Plot of the real and imaginary parts of the effective dynamic-dielectric-response function $\varepsilon_{\text{eff}}(\omega,q,L)$ versus $\hbar\omega/t_0$ for the three BN-DWNTs (17,0)@(25,0), (25,0)@(33,0), and (37,0)@(45,0). The wave number q and the angular momentum L are the same as in Fig. 3. The parameters Δ, t_0, and Γ, used to generate this figure, are given in the text. The open and solid circles mark the zeros of Re $\varepsilon_{\text{eff}}(\omega,q,L)$. The arrow on the horizontal axis indicates the location of the π-plasmon energy. The figure demonstrates a universality of the π-plasmon energy in the zigzag BN-DWNTs of different diameters.

(dispersion and damping) in the BN-DWNTs are not affected by the radii of the constituent BN-SWNTs, at least at small values of q and L. The result is consistent with that obtained in our previous paper[7] for individual zigzag BN-SWNTs and possibly can explain the observation by Arenal *at al.*[6] that three different BN-DWNTs, studied by the nonmomentum-resolved EELS method, appear to have had a dominant peak structure (of presumably π-plasmonic nature) in their EELS spectra at one and the same energy. However, because of the shortage of the experimental data presented in Ref. 6, on the one hand, and the limitations of the experimental method used in that paper, on the other hand, it is probably wise to be cautious about the above explanation.

Figure 5 shows the calculated $L=0$ π-plasmon spectrum for the BN-DWNT (17,0)@(25,0). For the sake of comparison, in the same figure we have also shown the almost complete merged branches of the $L=0$ π plasmons in the constituent BN-SWNTs (17,0) and (25,0). As seen from that figure, none of the branches start from $q=0$, the result that was pointed out in our previous paper[7] as being typical of that we have obtained for the π-plasmon dispersion in BN-SWNTs.[31] Figure 5 tells us that the same prominent feature is intrinsic to the $L=0$ π-plasmon branch of the collective electronic excitations in BN-DWNTs. The other branches of these excitations (with $L=1,2$) we have examined also start from a nonzero value of q (see Fig. 6 further below). However, the most important message of Fig. 5 is that BN-DWNTs can support the collective π-electronic excitations even at those values of the wave number q at which the π-plasmon modes do not exist in either of the constituent BN-SWNTs if the latter are considered separately, i.e., without taking account of the Coulomb coupling between them. Thus, we can conclude that an appreciable shift (toward smaller wave numbers) of the starting point of the $L=0$ π-plasmon dispersion curve in the BN-DWNT with regard to that in the constituent BN-SWNTs, observed in Fig. 5, is controlled by the Coulomb interaction between the electrons which are completely localized in two different shells of the

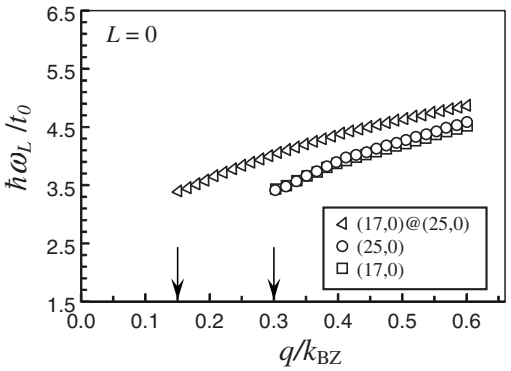

FIG. 5. The calculated dispersion curves for the $L=0$ π-plasmon modes in the BN-DWNT (17,0)@(25,0) (triangles) and in the two constituent BN-SWNTs (17,0) (squares) and (25,0) (circles). The arrows on the horizontal axis indicate the threshold values of the wave number q, at which the dispersion curves in the former and in the latter make their start. The parameters used to generate this figure are given in the text.

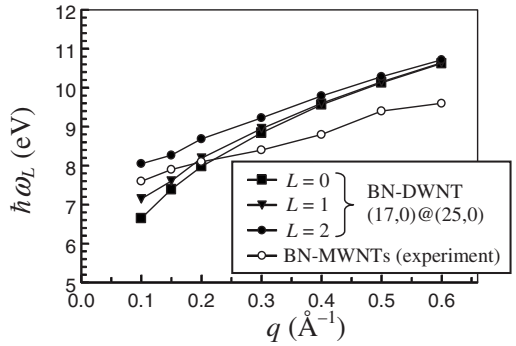

FIG. 6. The calculated energies $\hbar\omega_L$ of $L=0,1,2$ π-plasmon modes in the BN-DWNT (17,0)@(25,0) at several values of the wave number q are shown by solid squares, triangles, and circles, respectively. The open circles show the π-plasmon energies derived from the EELS experiment of Fuentes *et al.* (Ref. 5) on a sample of BN-MWNTs and presented in Fig. 6 in Ref. 5. The transfer integral t_0 between π orbitals of nearest-neighboring B and N atoms is chosen to be equal to 2 eV in order to give the best fit of our calculated results to those obtained experimentally in the above-mentioned paper. The solid lines are intended as a guide to the eye.

nanotube. This interaction produces one more noticeable effect, which is clearly seen in Fig. 5: namely, at those values of the wave number q at which the π plasmons can simultaneously exist in the BN-DWNT and in both the constituent BN-SWNTs, the π-plasmon dispersion curve in the former is significantly shifted (toward higher energies) relative to the π-plasmon dispersion curves in both the latter ones. Whether both the above-mentioned shifts are really measurable in momentum-resolved EELS experiment raises an interesting topic for future investigation.

Figure 6 shows a plot of the π-plasmon energy $\hbar\omega_L$ (in units of eV) versus the wave number q (in units of Å^{-1}), calculated for the BN-DWNT (17,0)@(25,0), chosen as a typical example, at the three different values of the angular momentum $L(=0,1,2)$. The grid in the q variable has been taken to be the same as in Ref. 5, where the loss spectra of the BN-MWNTs between 2 and 15 eV as a function of the transferred momentum q was measured by using the EELS method. The π-plasmon energies, derived from those spectra and presented in Fig. 6 in the above-mentioned paper, are also included for comparison in our Fig. 6. The calculated values of the plasmon damping factor $\gamma_L(q)/\omega_L(q)$ [see Eq. (27)] for the same grade of the q values as in Fig. 6 are given in Table I. It is clear from this table that the damping is small, i.e., the inequality of Eq. (26) is satisfied for all the three branches of the π-plasmon modes shown in Fig. 6 so that they really correspond to well-defined collective electronic excitations of the system under consideration.

It is instructive to compare the calculated and the experimental wave-number-dispersed π-plasmon energies in Fig. 6, even though such a comparison can hardly be recognized as being of full value. The point is that the experimental sample contained BN-MWNTs of different diameters and chiralities, whereas our model is formally relevant only to individual zigzag BN-DWNTs. Besides, due to the large area probed by the primary electron beam, the loss spectra, measured in Ref. 5, provide only average picture of plasmon properties. Nevertheless, based only on looking briefly at Fig. 6, it appears that our results are not in conflict with the experimental ones, at least at a general, qualitative level. In particular, the theory developed predicts a considerable positive wave-number dispersion of the π-plasmon modes with different L's, which is consistent with the experiment in Ref. 5, if we attribute the measured dispersive mode to one of an L π-plasmon with a small L. In spite of this overall qualitative agreement, one can see a systematic quantitative discrepancy between the experimental and the calculated π-plasmon energies in that figure, especially at large values of the wave number q (Ref. 32). It is generally not quite surprising in view of how different are the systems studied in this paper and in Ref. 5; one should rather be surprised that, in spite of this difference, the measure of disagreement, revealed in Fig. 6, is not so large as could be expected *a priori*. Thus, we can conclude that, although our results cannot be applied to BN-MWNTs straightforwardly, at a qualitative level they are able to account satisfactorily for the main features of the π-plasmon dispersion in those nanotubes. It is not quite unexpected since the results presented above prove that the π-plasmon energies in a special case of BN-DWNTs are not influenced by the radii of the constituent BN-SWNTs. This allows us to suggest, with some care, that the same is true in a general case of BN-MWNTs with the number of shells larger than two. If so, then the number of shells, as well as their diameters and possibly chiralities, are not crucial physical parameters that control the behavior of the π plasmons in BN-MWNTs.[33] Certainly, to make any firm deductions on this point, more precise measurements on samples of BN-MWNTs with a well-defined number of shells and carefully control chiral structure are needed. This seems to be an interesting and challenging experimental task. On the theoretical side, there is also a need for considerable further work to extend the theory, developed in this paper, to the case of BN-MWNTs with an arbitrary number of shells. This, along with a more sophisticated calculation going beyond the RPA and including the exchange-correlation effects, would make the comparison between theory and experiment more meaningful.[34] More refined calculations are also needed to include σ electrons in the theory in order to make it suitable for the description of the $\sigma+\pi$-plasmon modes, which manifest themselves as higher-energy peaks in the EELS experiment of Fuentes *et al.*[5] Finally, it seems to be an important task to check the predictions made above in momentum-resolved EELS experiments on individual BN-DWNTs and/or on samples containing only such nanotubes.

IV. CONCLUSIONS

To summarize, in this paper we have presented a theoretical treatment of the collective π-electronic excitations in individual BN-DWNTs consisting of two coaxial zigzag BN-SWNTs. Taking into account only the Coulomb interaction between the shells and neglecting the intershell electron tunneling, the effective dynamic-dielectric-response function of the system has been derived within the RPA using a field-theoretical method. We have obtained an explicit expression for this function in terms of the true dynamic-dielectric-

response functions of two constituent BN-SWNTs. Using a simple tight-binding model for the π-electronic band structure of the BN-SWNTs, developed in our previous paper,[7] we have numerically calculated the dispersion and damping of the π plasmons in the BN-DWNTs of fairly large diameters. In all the cases we have examined, the damping is small so that the π plasmons in the BN-DWNTs represent long-lived and hence well-defined collective electronic excitations supported by these systems.

The results, obtained for the spectrum of the π plasmons, show that, like the BN-SWNTs considered in Ref. 7, each of the BN-DWNTs supports only one branch of the wave-number-dispersed π-plasmon mode for each value of the angular momentum $L(=0,1,2,\ldots)$, all the dispersion curves starting from a nonzero value of the wave number q. We have also found that the π plasmons in the BN-DWNTs can exist even at those q values at which the π-plasmon modes are not supported by either of the constituent BN-SWNTs if the latter are considered separately, i.e., without taking into account the Coulomb coupling between them. In particular, we have found that the threshold value of the wavelength, at which the $L=0$ π-plasmon dispersion curve in the BN-DWNTs makes its start, is redshifted as compared to that in the constituent BN-SWNTs. Besides, at those values of the wave number q, at which the π plasmons can simultaneously exist in a BN-DWNT and in both the shells of the nanotube, the $L=0$ π-plasmon dispersion curve in the former is appreciably blueshifted relative to the π-plasmon dispersion curves in both the latter ones. Since both the above-mentioned shifts (in wavelength and in energy) are fairly large, we do not see any difficulties preventing their observation in momentum-resolved EELS experiment. If it were possible that way, it would serve as direct evidence of the importance of the intershell Coulomb coupling in BN-DWNTs.

Another important and experimentally testable conclusion, which results from our discussion, is that the π-plasmon energies in the BN-DWNTs are not affected by the main geometrical parameter of the constituent BN-SWNTs—namely, their diameter. This result implies that the π-plasmon energies, derived from our calculations for several selected zigzag BN-DWNTs, are not specific for only those nanotubes but are typical of the whole class of such tubules.

As remarked earlier, the present calculations were motivated by the two recent experimental EELS studies of BN-NTs.[5,6] For the reasons mentioned in Sec. III, a quantitative comparison of our theory with the experiments in Refs. 5 and 6 is unavoidable limited so that, in our view, it would be premature to make any firm deductions on the adequacy of the model used in this paper. However, some of the qualitative results obtained here are consistent with those experiments. This agreement is very encouraging confirmation of the fact that the above-mentioned model can serve as a useful paradigm to gain an insight into the π-plasmon characteristics in real BN-NT systems, suggesting a fertile theoretical background for future investigations. In this connection, it would be of great interest to see momentum-resolved EELS studies of the π plasmons in such systems as explored here. We hope that the results of the present paper will stimulate more vigorous experimental work in this direction.

ACKNOWLEDGMENTS

This work has been supported by the Russian Foundation for Basic Research through Grant No. 08-02-01035-a.

*Author to whom correspondence should be addressed; 612033@inbox.ru

[1] A. Rubio, J. L. Corkill, and M. L. Cohen, Phys. Rev. B **49**, 5081 (1994).
[2] A. Loiseau, F. Willaime, N. Demoncy, G. Hug, and H. Pascard, Phys. Rev. Lett. **76**, 4737 (1996).
[3] M. Terauchi, M. Tanaka, T. Matsumoto, and Y. Saito, J. Electron Microsc. **47**, 319 (1998).
[4] M. Kociak, L. Henrard, O. Stéphan, K. Suenaga, and C. Colliex, Phys. Rev. B **61**, 13936 (2000).
[5] G. G. Fuentes, E. Borowiak-Palen, T. Pichler, X. Liu, A. Graff, G. Behr, R. J. Kalenczuk, M. Knupfer, and J. Fink, Phys. Rev. B **67**, 035429 (2003).
[6] R. Arenal, O. Stéphan, M. Kociak, D. Taverna, A. Loiseau, and C. Colliex, Phys. Rev. Lett. **95**, 127601 (2005).
[7] Vl. A. Margulis, E. E. Muryumin, and E. A. Gaiduk, Phys. Rev. B **77**, 035425 (2008).
[8] H. Ehrenreich and M. H. Cohen, Phys. Rev. **115**, 786 (1959).
[9] M. S. Dresselhaus, G. Dresselhaus, and P. C. Eklund, *Science of Fullerenes and Carbon Nanotubes* (Academic, San Diego, 1996); R. Saito, G. Dresselhaus, and M. S. Dresselhaus, *Physical Properties of Carbon Nanotubes* (Imperial College, London, 1998).
[10] J. Cumings and A. Zettl, Chem. Phys. Lett. **316**, 211 (2000).
[11] M. Terrones, J. M. Romo-Herrera, E. Cruz-Silva, F. López-Urias, E. M. noz Sandoval, J. J. Velázquez-Salazar, H. Terrones, Y. Bando, and D. Golberg, Mater. Today **10**, 30 (2007).
[12] A. L. Fetter and J. D. Walecka, *Quantum Theory of Many-Particle Systems* (Dover, New York, 2003).
[13] H. Bruus and K. Flesberg, *Many-Body Quantum Theory in Condensed Matter Physics* (Oxford University Press, Oxford, 2004).
[14] D. Pines, *Elementary Excitations in Solids* (Benjamin, New York, 1963); D. Pines and P. Nozières, *The Theory of Quantum Liquids* (Addison-Wesley, New York, 1989).
[15] M. Terauchi, M. Tanaka, K. Suzuki, A. Ogino, and K. Kimura, Chem. Phys. Lett. **324**, 359 (2000).
[16] R. S. Lee, J. Gavillet, M. Lamy de la Chapelle, A. Loiseau, J. L. Cochon, D. Pigache, J. Thibault, and F. Willaime, Phys. Rev. B **64**, 121405(R) (2001).
[17] G. Y. Guo and J. C. Lin, Phys. Rev. B **71**, 165402 (2005).
[18] S. Okada, S. Saito, and A. Oshiyama, Phys. Rev. B **65**, 165410 (2002).
[19] T. M. Schmidt, R. J. Baierle, P. Piquini, and A. Fazzio, Phys. Rev. B **67**, 113407 (2003).

[20] H. J. Xiang, J. Yang, J. G. Hou, and Q. Zhu, Phys. Rev. B **68**, 035427 (2003).
[21] X. Blase, A. Rubio, S. G. Louie, and M. L. Cohen, Europhys. Lett. **28**, 335 (1994).
[22] L. D. Landau, E. M. Lifshitz, and L. P. Pitaevskii, *Electrodinamics of Continuous Media*, 2nd ed. (Pergamon, Oxford, 1984).
[23] C.-H. Park, C. D. Spataru, and S. G. Louie, Phys. Rev. Lett. **96**, 126105 (2006).
[24] L. Wirtz, A. Marini, and A. Rubio, Phys. Rev. Lett. **96**, 126104 (2006).
[25] A. G. Marinopoulos, L. Wirtz, A. Marini, V. Olevano, A. Rubio, and L. Reining, Appl. Phys. A: Mater. Sci. Process. **78**, 1157 (2004).
[26] R. Perez and W. Que, J. Phys.: Condens. Matter **18**, 3197 (2006).
[27] Vl. A. Margulis, E. A. Gaiduk, E. E. Muryumin, O. V. Boyarkina, and L. V. Fomina, Phys. Rev. B **74**, 245419 (2006).
[28] J. S. Lauret, R. Arenal, F. Ducastelle, A. Loiseau, M. Cau, B. Attal-Tretout, and E. Rosencher, Phys. Rev. Lett. **94**, 037405 (2005).
[29] J. Wang, V. K. Kayastha, Y. K. Yap, Z. Fan, J. G. Lu, Z. Pan, I. N. Ivanov, A. A. Puretzky, and D. B. Geohegan, Nano Lett. **5**, 2528 (2005).
[30] G. Y. Guo, S. Ishibashi, T. Tamura, and K. Terakura, Phys. Rev. B **75**, 245403 (2007).
[31] Note that this feature is not a unique property of only the collective excitations in BN-NTs. For metals (such as sodium), the occurence of the specific interband collective electronic modes, the so-called zone-boundary collective modes, which, unlike conventional plasmonic modes, do not exist at small values of the wave vector, was pointed out by E-Ni Foo and J. J. Hopfield, Phys. Rev. **173**, 635 (1968) a long time ago. However, as a matter of fact, such modes are experimentally observed only in noble and transition metals. In alkali metals, the peaks of the energy-loss function, associated with those modes, manifest themselves only in experiments on monocrystals [see, e.g., C. H. Chen and J. Silcox, Phys. Rev. B **16**, 4246 (1977)], having thereby very small intensity as compared to that of the main plasmon-resonance peak.
[32] Obviously, as q increases our theoretical results become less reliable because the RPA, which we have rilied on in this paper, is applicable, strictly speaking, only if $q \ll k_{BZ}$, i.e., at a small transfer momentum. We believe, however, that the results obtained should be qualitatively valid even as q approaches the one-dimensional-Brillouin-zone edge of the nanotube. What may militate in favor of this latter is the excelent agreement between the RPA theory [E. H. Hwang and S. Das Sarma, Phys. Rev. B **64**, 165409 (2001)] and the experiment; [M. A. Eriksson, A. Pinczuk, B. S. Dennis, C. F. Hirjibehedin, S. H. Simon, L. N. Pfeiffer, and K. W. West, Physica E (Amsterdam) **6**, 165 (2000)] on collective excitations in GaAs quantum wells at very low carrier densities and very large wave vectors. The above-mentioned statement is also strongly supported by a theoretical analysis of the dynamic response of a one- dimensional quantum-wire electron system; [S. Das Sarma and E. H. Hwang, Phys. Rev. B **54**, 1936 (1996)], which convincingly proves that the RPA description of plasmon dispersion works better in one-dimensional systems than in two- and three-dimensional ones.
[33] Recently, M. H. Upton, R. F. Klie, J. P. Hill, T. Gog, D. Casa, W. Ku, Y. Zhu, M. F. Sfeir, J. Misewich, G. Eres, and D. Lowndes, arXiv:cond-mat/0611151 (unpublished) have arrived at the same conclusion in the case of CNTs, carrying out momentum-resolved EELS measurements on a number of isolated double-walled CNTs, as well as on samples of aligned multiwalled and aligned few-walled CNTs.
[34] It is worthwhile to note, however, that, as is known by experience accumulated over the years in many-particle physics, a more involved approach does not necessarily lead to better results. A notable example of such a situation is the theory of the collective excitations in a low-density two-dimensional electron system, developed by Hwang and Das Sarma (see Ref. 32). The calculation of the plasmon dispersion, carried out by those authors, shows that the RPA offers much better agreement with the experiment, cited in Ref. 32, as compared to its "improved" version including local-field corrections arising from correlation effects.